

## Ab Initio Models for the Nitroaldol (Henry) Reaction

Begoña Lecea, Ana Arrieta, Iñaki Morao, and Fernando P. Cossío\*

**Abstract:** Ab initio calculations (up to MP4SDQ/6-31 + G\*\*//MP2(FU)/6-31 + G\* +  $\Delta$ ZPVE) on several model nitroaldol (Henry) reactions have been performed. It is found that the free nitronate anions react with aldehydes via transition states in which the nitro and carbonyl dipoles are antiperiplanar to each other. This kind of reaction yields *anti* (*erythro*) nitroalcohols as major products. The Henry reaction between lithium nitronates and aldehydes is predicted to occur via cyclic transition structures yielding *syn* nitroalcohols as major products. The stereocontrol in these model reactions is low. The factors affecting the stereoselectivity in the reaction between dilithiated nitronates and aldehydes are also discussed.

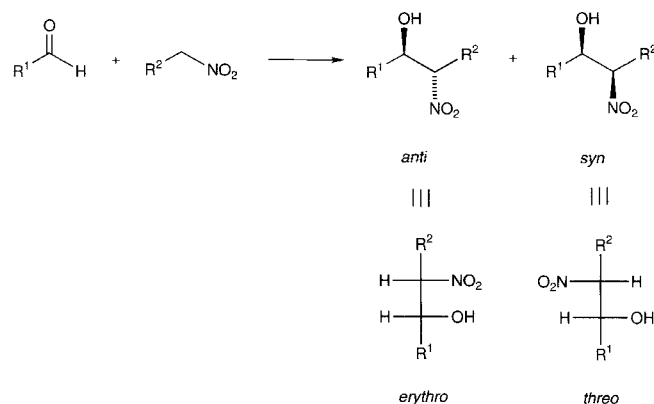
### Keywords

ab initio calculations · Henry reaction · nitroaldol reactions · reaction mechanisms

### Introduction

The nitroaldol reaction between a nitroalkane and a carbonyl compound to yield a nitroalcohol was discovered in 1895 by Henry.<sup>[1]</sup> Since then, this reaction has become a classical method for the chemical synthesis of carbon–carbon bonds, and has been used in the synthesis of diverse naturally occurring or biologically interesting products.<sup>[2]</sup> In addition, the versatility of the nitro group provides a facile entry to a wide range of functional groups starting from the nitroalcohol products.<sup>[3]</sup> In view of its significance, the scope and usefulness of the nitroaldol reaction has been extensively reviewed,<sup>[4]</sup> although the development of this reaction is less advanced than that achieved for the aldol reaction. In particular, the stereochemical problem of this reaction is still challenging in many cases.

The Henry reaction between a primary nitroalkane and an aldehyde can yield the corresponding *anti* (*erythro*) and *syn* (*threo*) isomers (Scheme 1). Seebach and co-workers<sup>[5]</sup> have developed complementary protocols that allow either *syn* or *anti* diastereomers to be formed preferentially. Thus, silyl nitronates generally<sup>[6]</sup> yield *anti* nitroalcohols. In contrast, double deprotonation of nitroalkanes or nitroalcohols with lithium bases followed by reprotonation preferentially yields the corresponding *syn* diastereomers; if the reprotonation is carried out with  $\alpha$ -silyloxy lithium nitronates the *anti* nitroalcohol is again the major product. On the other hand, several groups have reported



Scheme 1. Possible diastereomers formed by the Henry reaction between a primary nitroalkane and an aldehyde (only one enantiomer is drawn).

preferential *anti* stereocontrol in the Henry reaction using neutral alumina<sup>[7]</sup> or tetrabutylammonium fluoride<sup>[8]</sup> (TBAF) as reagent or catalyst, respectively. Finally, it is noteworthy that *syn* stereocontrol has been reported for the Henry reaction catalyzed by lanthanum–lithium complexes.<sup>[9]</sup>

In spite of its significance, the Henry reaction has not, to the best of our knowledge, been explored by means of high-level computational tools. We present herein an ab initio SCF-MO study on the Henry reaction, in the hope that the models thus developed could be useful in the design of new versions of this reaction.

### Computational Methods

All the calculations reported in this work were performed with GAUSSIAN 92 [10] or GAUSSIAN 94 [11] packages. Given the presence of species bearing significant negative charge along the reaction coordinates under

[\*] Prof. F. P. Cossío, Prof. A. Arrieta, I. Morao  
Kimika Fakultatea, Euskal Herriko Unibertsitatea  
P. K. 1072, 20080 San Sebastián-Donostia (Spain)  
Fax: Int. code +(43)212-236  
e-mail: qopcomof@sq.ehu.es

Prof. B. Lecea  
Farmazi Fakultatea, Euskal Herriko Unibertsitatea  
P. K. 450, 01080 Vitoria-Gasteiz (Spain)

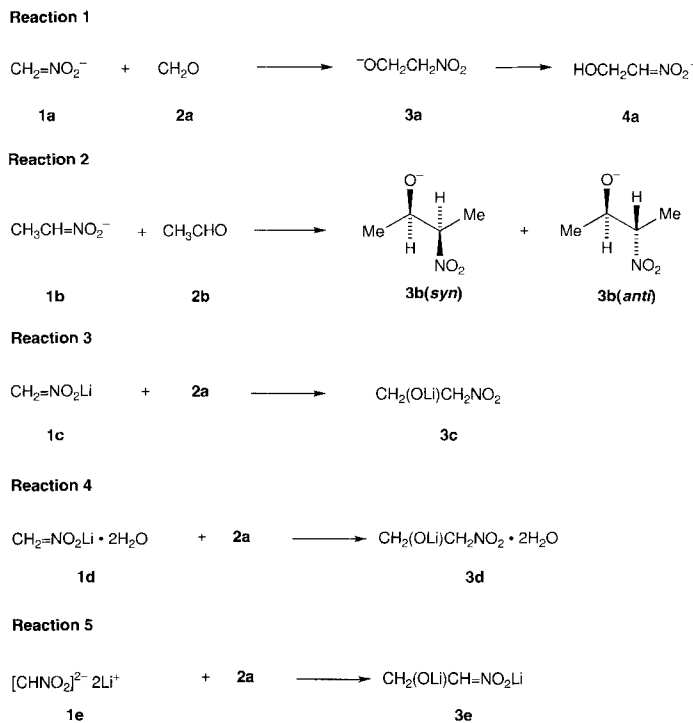
study, we used the 6-31 + G\* basis set [12]. Electron correlation was partially taken into account by using the Møller–Plesset method [13]. Both full core (FU) and frozen core (FC) approximations were used [14]. However, both approaches yielded similar results for the relative energies corresponding to the stationary points included in our study. Therefore, unless otherwise stated, the MP2 data correspond to the frozen core approach. In some cases density-functional theory (DFT) was used [15], in order to introduce electron correlation during the geometry optimization of relatively large structures. Approximate DFT calculations were carried out by using a hybrid three-parameter functional developed by Becke [16], which combines the Becke's gradient-corrected exchange functional and the Lee–Yang–Parr and Vosko–Wilk–Nusair correlation functionals [17] with part of the exact Hartree–Fock exchange energy. This hybrid functional will be denoted as B3LYP. Zero-point vibrational energies (ZPVE) were computed at either HF/6-31 + G\* or MP2/6-31 + G\* and scaled with the 0.89 and 0.96 correction factors, respectively [18]. The B3LYP results were not scaled. Stationary points were characterized by frequency calculations [19]. All reactants, reaction intermediates and products have positive defined Hessian matrices. All transition structures (TSs) show only one negative eigenvalue in their diagonalized force constant matrices, and their associated eigenvectors were confirmed to correspond to motion along the reaction coordinate under consideration. For several reactions intrinsic reaction coordinate [20] (IRC) calculations were performed to connect previously computed transition structures with reaction intermediates and products. No symmetry constraints were imposed during the optimizations. Atomic charges [21] and bond indices [22] were calculated by the natural bonding analysis (NBA) method [23]. All calculations involving the atoms-in-molecules theory developed by Bader [24] were performed with the AIMPAC package [25].

## Results and Discussion

As model systems we studied the interaction between nitronates derived from nitromethane or nitroethane and simple aldehydes, such as formaldehyde and acetaldehyde. These reactions are shown in Scheme 2. The energetics and the geometries of the different reaction pathways associated with reactions 1–5 are collected in Tables 1–6 and in Figures 2–8, respectively. The definition of the relative energies discussed in this section is indicated in Figure 1. In the following subsections we shall present and discuss separately the results obtained for each of these reactions.

**Nitromethane Nitronate plus Formaldehyde (Reaction 1):** The relevant differences in energy corresponding to this reaction are given in Table 1, and the fully optimized stationary points are depicted in Figure 2. Nitromethane nitronate (**1a**) is predicted

**Abstract in Basque:** Nitroaldol (Henry) erreakzioaren eredu desberdinen ab initio kalkuluak (MP4SDQ/6-31 + G\*/MP2(FU)/6-31 + G\* + ΔZPVE teoria-mailaraino) egin dira. Nitronato anioi askeek aldehidoekin erreakzionatzen dutela ikusi da, nitro eta karbonil dipoloak elkarrekiko antiperiplanar leudekeen trantsiziozko egoeren bitartez. Erreakzio mota honek anti (erithro) nitroalkoholak ematen ditu produktu nagusi. Litio nitronato eta aldehidoen arteko Henry erreakzioa trantsiziozko egitura ziklikoan bitartez gertatzen dela aurresaten da, produktu nagusi syn nitroalkoholak emanez. Erreakzio hauetan estereokontrola baxua da. Bilitiodun nitronato eta aldehidoen arteko erreakzioaren estereoselektibitatean eragina duten faktoreak ere eztabaidatzen dira.



Scheme 2. The five Henry reactions studied in this work.

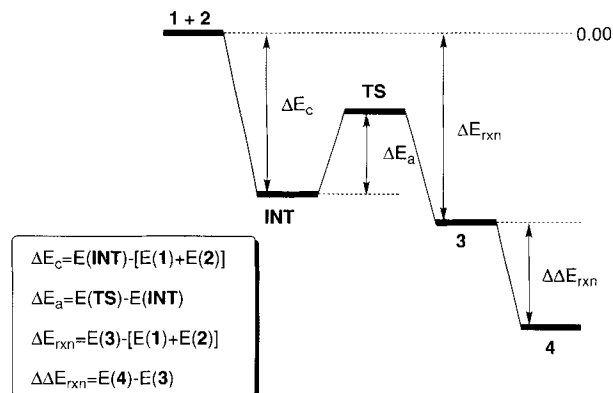


Figure 1. Definition of the relative energies used in the present work. Structures 1–4 are defined in Scheme 2. The same substitution patterns apply to intermediates INT and saddle points TS.

to be a planar  $C_{2v}$ -symmetric anion at both HF/6-31 + G\* and MP2(FU)/6-31 + G\* levels of theory, in agreement with the data reported by Wiberg.<sup>[26]</sup> Interaction of **1a** with formaldehyde **2a** leads without any activation barrier to the complex **INTa** (Figure 2). This complex also has  $C_{2v}$  symmetry and lies 13.47 kcal mol<sup>-1</sup> below the reactants at the MP4SDQ/6-31 + G\*/MP2(FU)/6-31 + G\* + ΔZPVE level. The saddle point **TSa** associated with the C–C bond forming step has  $C_s$  symmetry, with a O6–C5–C2–N1 dihedral angle  $\omega$  of ca. 180° at both HF/6-31 + G\* and MP2(FU)/6-31 + G\* levels. **TSa** and **INTa** were confirmed to be associated with the same process by means of an IRC analysis starting from **TSa**.<sup>[27]</sup> The geometry of this saddle point involves an antiperiplanar relative orientation between the nitronate and carbonyl dipoles. The C2–C5 distance is 2.292 Å at the latter level, a value similar to those calculated for both sequential and pericyclic reactions involving formation

Table 1. Differences in energy [a,b] (kcal mol<sup>-1</sup>) corresponding to reaction 1, Scheme 2 (nitromethane nitronate + formaldehyde).

	HF/6-31+G*	MP2(FU)/6-31+G*// HF/6-31+G*	MP2(FU)/6-31+G*	MP3/6-31+G*// MP2(FU)/6-31+G*	MP4SDQ/6-31+G*// MP2(FU)/6-31+G*
$\Delta E_c$	-13.16	-13.37	-13.06	-7.79	-13.47
$\Delta E_{zpe}$	+15.66	+2.99	+2.28	+7.17	+6.88
$\Delta E_{rxn}$	-5.05	-14.51	-15.83	-4.56	-12.22
$\Delta\Delta E_{rxn}$	-10.96	-10.52	-9.04	-14.90	-10.57

[a] See Figure 1 for the definition of energy differences. [b] Zero-point vibrational energies are included.

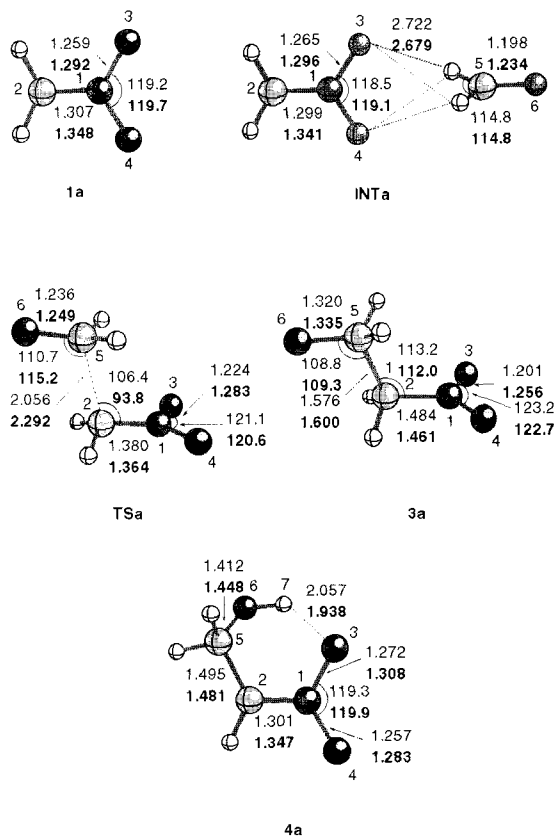


Figure 2. Fully optimized stationary points located in the reaction between nitromethane nitronate and formaldehyde, computed at the HF/6-31+G\* and MP2(FU)/6-31+G\* (bold numbers) level. In this, and the remaining figures showing ball-and-stick representations, unless otherwise stated, atoms are represented by increased shading in the following order: H, C, N, and O. Bond lengths and angles are given in Å and deg, respectively.

of C–C bonds.<sup>[28, 29]</sup> The C2–C5 bond index is 0.417, and the NBA reveals that the formaldehyde moiety bears a net charge of  $-0.34$  at the expense of the nitronate. These results are compatible with a nearly “halfway”, although slightly early transition structure. It is also interesting to note that the angle (C2–C5–O6) of attack over the  $sp^2$  carbon of the aldehyde ( $\alpha_N$ ) is  $115.2^\circ$  at the MP2(FU)/6-31+G\* level. The analogous angle associated with the nitronate  $\alpha'_N$  (C5–C2–N1) is found to be  $93.8^\circ$  at the same level. The former value is in the range of the angles of attack associated with the Bürgi–Dunitz trajectory.<sup>[30]</sup> We have not been able to locate TSs with a *gauche* relationship between the alkoxide oxygen and the nitro group. This result is not surprising, since a strong Coulombic repulsion between the two groups is to be expected for these hypothetical saddle points. At our highest level of theory, the Henry reaction between nitromethane nitronate and formaldehyde in the gas

phase has an activation barrier from the complex INTa of  $6.88$  kcal mol<sup>-1</sup>. This value lies between the HF/6-31+G\* and the MP2(FU)/6-31+G\* results.

The reaction product **3a** is calculated to be  $12.22$  kcal mol<sup>-1</sup> more stable than the reactants **1a** and **2a** at our highest level of theory (see Table 1). It is interesting to note that our calculations yield  $\Delta E_{rxn}$  values that are comparable to those obtained for  $\Delta E_c$ . Indeed, the C–C bond forming step is slightly endothermic at the MP4SDQ/6-31+G\*//MP2(FU)/6-31+G\* level. As a consequence, although the reaction as a whole is exothermic, the step corresponding to the formation of the C–C bond is reversible, and it is likely that this effect would be more pronounced in solution. We have also found, however, that the nitroalkoxide **3a** can isomerize to the hydroxynitronate **4a** (Figure 2). The latter is ca.  $11$  kcal mol<sup>-1</sup> more stable than **3a** (see the  $\Delta\Delta E_{rxn}$  values in Table 1), and has a pseudocyclic structure, because of strong hydrogen bonding between the H7 and O3 atoms. In fact, the shape of **4a** is rather similar to that of 2-nitroethanol, although the intramolecular hydrogen bond is obviously weaker in the latter (Figure 3a). Therefore, **4a** can act as an energy trap and shifts the equilibrium toward the nitroaldol products. In addition, this nitronate is thought to be involved in

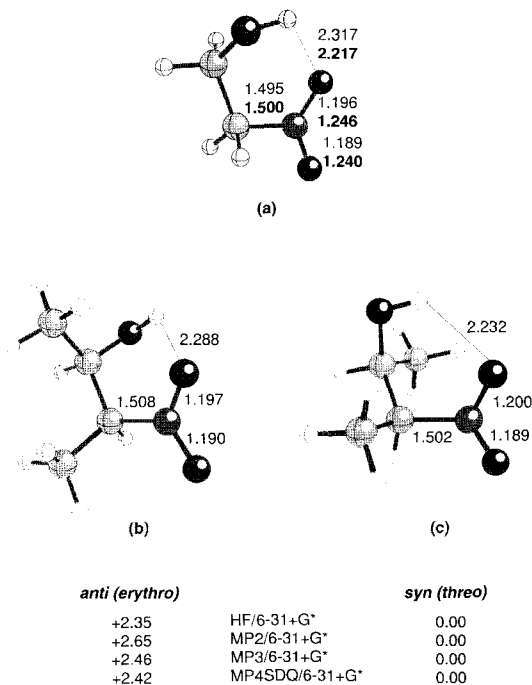


Figure 3. Fully HF/6-31+G\* and MP2(FU)/6-31+G\* (bold numbers) optimized structures of a) 2-nitroethanol, b) *anti*-3-nitro-2-butanol, and c) *syn*-3-nitro-2-butanol. Distances are given in Å. Relative energies (kcal mol<sup>-1</sup>), computed at several theoretical levels on HF/6-31+G\* geometries, are also included.

Table 2. Differences in energy [a,b] (kcal mol<sup>-1</sup>) corresponding to reaction 2, Scheme 2 (nitroethane nitronate plus acetaldehyde).

	HF/6-31 + G*	MP2/6-31 + G*// HF/6-31 + G*	MP3/6-31 + G*// HF/6-31 + G*	MP4SDQ/6-31 + G*// HF/6-31 + G*
$\Delta E_c$	-12.81	-14.26	-6.35	-5.53
$\Delta E_a(\text{syn})$	+20.80 (0.00) [c]	+4.42 (0.00) [c]	+11.86 (0.00) [c]	+10.97 (0.00) [c]
$\Delta E_a(\text{anti})$	+20.87 (-0.26) [c]	+4.59 (-0.16) [c]	+11.96 (-0.23) [c]	+11.08 (-0.22) [c]
$\Delta E_{\text{rel}}(\text{syn})$	+1.68 (0.00) [c]	-12.31 (0.00) [c]	+0.62 (0.00) [c]	-0.19 (0.00) [c]
$\Delta E_{\text{rel}}(\text{anti})$	+0.34 (-1.50) [c]	-13.51 (-1.36) [c]	-0.64 (-1.42) [c]	-1.45 (-1.42) [c]

[a] See Figure 1 for the definition of energy differences. [b] Zero-point vibrational energies, scaled by 0.89 and computed at the HF/6-31 + G\* level, are included. [c] Relative free energies (computed at 298.14 K with HF/6-31 + G\* thermochemical data) with respect to the formation of the *syn* adduct.

polyalkylation reactions,<sup>[4]</sup> although substituted nitronates such as **4a** are expected to be less reactive than **1a** itself (vide infra).

**Nitroethane Nitronate plus Acetaldehyde (Reaction 2):** The next step in our study was to explore the Henry reaction between monosubstituted nitronates and simple alkyl aldehydes. We chose acetaldehyde **2b** and the nitronate **1b** derived from nitroethane as model substrates. The geometries of the stationary points located for this reaction are reported in Figure 4, and the corresponding relative energies are given in Table 2.

The complex associated with the reaction coordinate is **INTb**. The complexation energy  $\Delta E_c$  for **INTb** is only  $-5.53$  kcal mol<sup>-1</sup> at our highest level of theory (Table 2), a value significantly lower than that computed for the parent reaction. The saddle

points associated with the formation of the C3–C4 bond are **TSb(anti)** and **TSb(syn)**, leading to the corresponding *erythro* and *threo* nitroaldols, respectively. It is found that **1b** is less nucleophilic than **1a**, and that the activation energies from **INTb** are ca. 11 kcal mol<sup>-1</sup> at the MP4SDQ/6-31 + G\*//HF/6-31 + G\* level, a value ca. 4 kcal mol<sup>-1</sup> higher than that obtained for the parent reaction. However, the shape of saddle points **TSb** is very similar to that of **TSa** (Figure 1). In particular, the relative orientation of the dipoles associated with the carbonyl and nitro groups remains virtually antiparallel. Quite surprisingly, the energy of **TSb(anti)** is calculated to be slightly higher than that of **TSb(syn)**,<sup>[31]</sup> although the relative energies are very close to each other. However, inclusion of vibrational enthalpy and total entropy corrections leads to a difference in free energy (298.14 K) of 0.22 kcal mol<sup>-1</sup> at the MP4SDQ/6-31 + G\*//HF/6-31 + G\* +  $\Delta ZPVE + \Delta H_{\text{vib}} + \Delta S$  level, where **TSb(anti)** is the saddle point of lowest energy. This result is in agreement, from the point of view of stereocontrol, with the observation that the counterion of the nitronate usually only plays a marginal or negligible role in Henry reactions.<sup>[4, 5, 8b]</sup> The higher energy of the *syn* TS probably arises from the *gauche* relationship between the alkyl (or aryl) substituents, since the alkoxy and nitro groups should be antiperiplanar to each other. The TSs associated with these reactions would then have the general geometry shown in Scheme 3. The stereocontrol in these Henry reactions is expect-

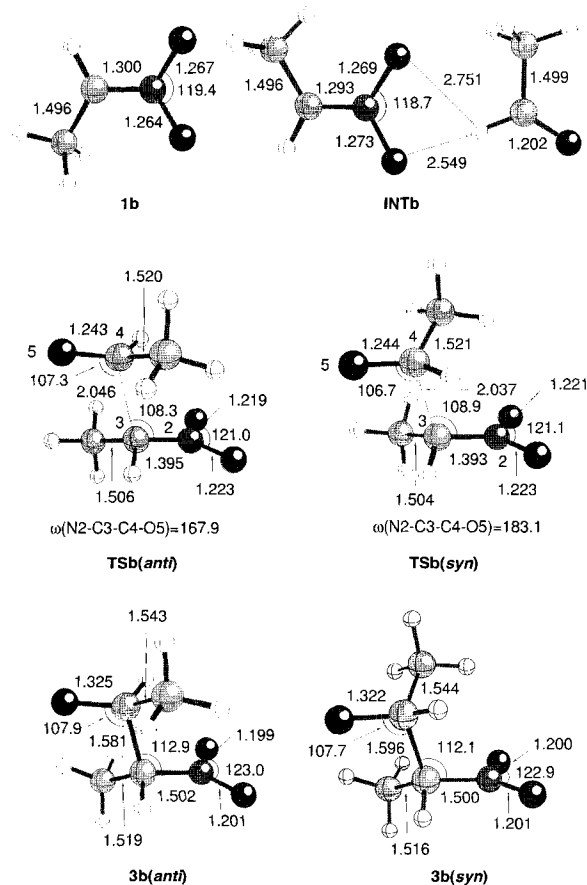
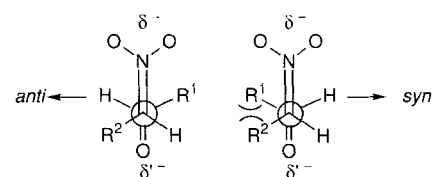


Figure 4. Fully optimized (HF/6-31 + G\* level) geometries of stationary points corresponding to reaction 2 (Scheme 2). Bond lengths and angles are given in Å and deg, respectively. Dihedral angles are given in absolute value.



Scheme 3. Possible geometries of transition states associated with the reactions of monosubstituted nitronates with aldehydes.

ed to depend upon the size of substituents R<sup>1</sup> and R<sup>2</sup>. It is also noteworthy that the geometry of these transition states closely resembles the structure of the hapten developed by Schultz et al.<sup>[32]</sup> for an antibody-catalyzed retro-Henry reaction.

The geometries of the products **3b(anti)** and **3b(syn)** are depicted in Figure 4. As expected, the shape of these nitroalkoxides is similar to that of **3a**. Since the *gauche* interactions between the methyl groups in **3b(syn)** are higher than in **TSb(syn)**, the difference in energy between the two diastereomers of **3b** is more pronounced than in the saddle points **TSb**. This difference in free energy is computed to be 1.42 kcal mol<sup>-1</sup> at our highest level of theory, with the *anti* alkoxide being more stable. However, the corresponding neutral *syn* nitroalcohol is found to be

Table 3. Differences in energy [a,b] (kcal mol<sup>-1</sup>) corresponding to reaction 3, Scheme 2 (nitromethane lithium nitronate plus formaldehyde).

	HF/6-31+G*	MP2/6-31+G*// HF/6-31+G*	MP2/6-31+G*	MP3/6-31+G*// MP2/6-31+G*	MP4SDQ/6-31+G*// MP2/6-31+G*
$\Delta E_c$	-16.70	-17.83	-17.61	-17.93	-17.64
$\Delta E_a$	+28.96	+16.82	+11.14	+20.81	+19.93
$\Delta E_{rxn}^{\ddagger}$	-5.74	-15.17	-16.28	-10.35	-11.31

[a] See Figure 1 for the definition of energy differences. [b] Zero-point vibrational energies, scaled by 0.89 and computed at the HF/6-31+G\* level, are included.

ca. 2.5 kcal mol<sup>-1</sup> more stable than its *anti* isomer, because of the presence of intramolecular hydrogen bonds, which stabilize pseudocyclic structures for these compounds (Figure 3 b,c).

Finally, it is worth mentioning that our calculations suggest that the reaction between nitronate **1b** and acetaldehyde (**2b**) is approximately thermoneutral, the value of  $\Delta E_{rxn}$  being only -1.45 kcal mol<sup>-1</sup> for the *anti* nitroalkoxide at our highest level of theory. We can therefore conclude that the Henry reaction between substituted nitroalkanes and carbonyl compounds is more difficult than the parent reaction from both kinetic and thermodynamic standpoints. This result is in agreement with the difficulties observed in Henry reactions between highly substituted carbonyl compounds and/or nitronates.<sup>[4]</sup>

**Nitromethane Lithium Nitronate plus Formaldehyde (Reaction 3):** This model reaction was selected to explore the effect of a metallic center along the reaction coordinate. The geometries of the stationary points located are collected in Figure 5, and the associated relative energies are reported in Table 3.

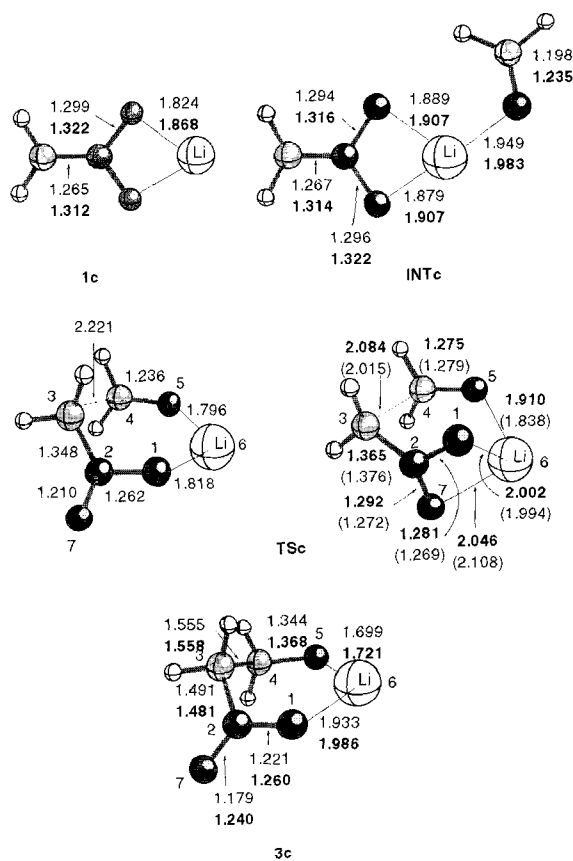


Figure 5. Fully HF/6-31+G\*, MP2(FC)/6-31+G\* (bold numbers), and B3LYP/6-31+G\* (numbers in parentheses) optimized geometries of stationary points corresponding to reaction 3 (see Scheme 2). Distances are given in Å.

We first optimized the structure of nitromethane lithium nitronate at both HF/6-31+G\* and MP2/6-31+G\* levels. According to our results, monomeric **1c** is predicted to have  $C_{2v}$  symmetry. The general features of this stationary point are in agreement with X-ray data available for a recently described symmetric potassium nitronate.<sup>[33]</sup> Boche et al. have reported the crystal structure of the polymeric aggregate [ $\alpha$ -nitrobenzyl-lithium-ethanol]<sub>n</sub>,<sup>[34]</sup> as a model for lithium nitronate/protic solvent interaction. This complex has an infinite ribbonlike structure including Li-O-N-O-Li-O six-membered rings. In our study, however, we considered only the reaction with monomeric lithium species. Previous computational studies<sup>[28, 35]</sup> suggest that models based upon monomeric enolates account reasonably well for the main features of the reaction between enolates and electrophilic double bonds. The reaction profiles associated with oligomeric structures will be the subject of further work. Our calculations on **1c** indicate that the interaction between the lithium atom and the oxygen atoms of the nitro group is electrostatic in nature. Thus, the energy density [ $H(r_c)$ ] at the critical points of the Li-O bond yields a positive value, namely,  $H(r_c) = +0.014$  au, which is indicative of an ionic bond.<sup>[36, 37]</sup> Moreover, the presence of the lithium cation has a significant effect on the nitronate counterion.<sup>[38]</sup> Thus, our calculations on **1c** at the MP2/6-31+G\* level yield a C=N bond length of 1.312 Å, whereas in **1a** this value is 1.348 Å. A complementary increase in the N-O bond lengths is observed from **1a** to **1c**. The NBA charge at the C atom in **1c** is -0.190, whereas in **1a** it is -0.471. The oxygen atoms of the nitronate moiety in **1c** and **1a** have NBA charges of -0.795 and -0.707, respectively. These results indicate that the Coulombic interaction between the nitronate and the lithium cation promotes a higher localization of the charge at the oxygen atoms, and the carbon atom of the nitronate is therefore less nucleophilic. Schleyer et al. have observed a similar effect in acetaldehyde enolates.<sup>[39]</sup>

We also located a complex **INTc**, formed from the interaction between **1c** and formaldehyde. This complex lies 17.64 kcal mol<sup>-1</sup> below the reactants at our highest level of theory (Table 3). Complexes of this type have been reported in the reaction between enolates and electrophiles,<sup>[28, 40]</sup> and in some cases crystallographic structural data are available.<sup>[41]</sup> It is noteworthy that our calculations at both the HF/6-31+G\* and MP2/6-31+G\* levels on **INTc** yield a structure in which formaldehyde interacts with **1c** through a lone pair instead of through the dipole (Figure 5). This result contrasts with those of other calculations on lithium complexation with aldehydes, in which linear structures are predicted.<sup>[28, 40, 42]</sup>

The transition structure associated with this reaction is **TSc** (Figure 5). At the HF/6-31+G\* level, this saddle point shows a sofa conformation, the Li6, O1, C2, C4, and O5 atoms being nearly coplanar. It is noteworthy that the lithium atom is only

Table 4. Relative energies [a,b] (kcal mol<sup>-1</sup>) of the transition structures depicted in Figure 6.

TS	Isomer	HF/6-31+G*	MP2/6-31+G*// HF/6-31+G*	MP3/6-31+G*// HF/6-31+G*	MP4SDQ/6-31+G*// HF/6-31+G*	B3LYP/6-31+G*
<b>TS<sub>ee</sub></b>	<i>syn</i>	0.00 (0.00)	0.00 (0.00)	0.00 (0.00)	0.00 (0.00)	0.00 [0.00]
<b>TS<sub>ea</sub></b>	<i>anti</i>	0.27 (0.23)	0.43 (0.46)	0.28 (0.25)	0.32 (0.28)	0.17 [0.35]
<b>TS<sub>ae</sub></b>	<i>anti</i>	0.97 (1.22)	0.03 (0.28)	0.33 (0.58)	0.23 (0.48)	0.65 [1.33]
<b>TS<sub>aa</sub></b>	<i>syn</i>	0.88 (1.02)	0.08 (0.23)	0.25 (0.40)	0.14 (0.28)	1.44 [1.88]

[a] Numbers in parentheses correspond to differences in free energy computed at 298.14 K with HF/6-31+G\* thermochemical data. [b] Numbers in square brackets correspond to differences in free energy computed at 298.14 K with B3LYP/6-31+G\* thermochemical data.

coordinated to one oxygen of the nitro group (O1 in Figure 5). This saddle point is similar to those reported for aldol reactions involving lithium enolates.<sup>[28, 40, 43]</sup> The bond index between C3 and C4 is 0.307 at the HF/6-31+G\* level, a value lower than those found for **TS<sub>a</sub>** and **TS<sub>b</sub>**. However, the shape of **TS<sub>c</sub>** is quite different at the MP2/6-31+G\* and B3LYP/6-31+G\* levels, as can be seen by inspection of Figure 5. This saddle point exhibits a distorted chairlike geometry, in which lithium is coordinated to the three oxygen atoms. In particular, the bond lengths Li6–O1 and Li6–O7 are quite similar to each other, and the absolute values of the dihedral angles between the N2, C3, C4, and O5 atoms are 27.5 and 21.7° at the MP2/6-31+G\* and B3LYP/6-31+G\* levels, respectively. The activation energies from **INT<sub>c</sub>** and from the separate reactants are 19.93 and 2.29 kcal mol<sup>-1</sup>, respectively (MP4SDQ/6-31+G\*//MP2/6-31+G\*+ΔZPVE data, Table 3). These values are significantly higher than those obtained for the Henry reaction involving the free nitronate (vide supra). It is to be expected that this lower reactivity of **1c** would be less significant in a solvated system. This particular aspect will be discussed below.

Finally, we characterized the reaction product **3c**, in which the chief geometric features of **TS<sub>c</sub>** at HF/6-31+G\* level, namely, sofa conformation and bicoordination of lithium, are preserved at both HF/6-31+G\* and MP2/6-31+G\* levels. The reaction **1c** + **2a** → **3c** is predicted to be exothermic, the Δ*E*<sub>rxn</sub> values being comparable to those computed for reaction 1 (see Tables 1 and 3). These values are lower than those reported for lithium-mediated aldol reactions.<sup>[44]</sup>

We also computed the transition structures associated with the Henry reaction between the lithium nitronate of nitroethane and acetaldehyde. Given the size of these systems and the convergence of the MP2/6-31+G\* and B3LYP/6-31+G\* results obtained for **TS<sub>c</sub>**, the geometry optimizations were performed only at the HF/6-31+G\* and B3LYP/6-31+G\* levels. The resulting structures of these saddle points are reported in Figure 6, and their relative energies are collected in Table 4. In contrast to the results obtained for **TS<sub>c</sub>**, the geometrical features of these latter saddle points are quite similar at both HF and B3LYP levels. In particular, the lithium atom is strongly coordinated to only one oxygen of the nitro group even at the B3LYP level. This is because the tricoordinated structure of **TS<sub>c</sub>** at the MP2 or B3LYP levels (Figure 5) induces a partial eclipsing between the methylene protons at C2 and C3. In the case of the TSs included in Figure 6, the presence of the bulkier methyl groups favors sofa geometries in order to minimize the Pitzer strain. Therefore, the tricoordinated geometry of **TS<sub>c</sub>** seems to be particular to the simplest case, that is, to the **1c** + **2a** → **3c** process. According to our calculations, the TS of lowest energy is associated

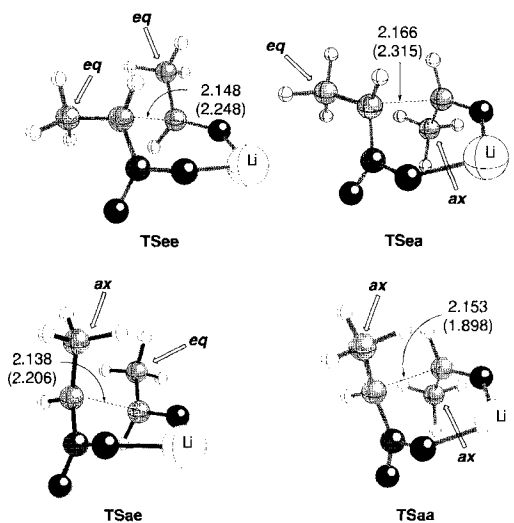


Figure 6. Fully HF/6-31+G\* and B3LYP/6-31+G\* (in parentheses) optimized geometries of transition structures associated with the C–C bond forming step in the reaction between nitroethane lithium nitronate and acetaldehyde. Distances are given in Å.

with the *syn* diastereomer, although the stereocontrol in this model reaction is quite low. It seems likely that increasing the bulk of the substituents of the reactants or that of the ligands bound to the metal would result in a higher stereocontrol in favor of the *syn* nitroaldols.

**Solvated Nitromethane Lithium Nitronate plus Formaldehyde (Reaction 4):** We selected this model reaction in order to explore the solvation effects on the metal-assisted Henry reaction. We found two solvated complexes for lithium nitronate **1c**. The first one, denoted as **INT<sub>d</sub>** in Figure 7, has two water molecules (as models for an ether solvent) interacting with the lithium atom. The energy density at the critical points associated with the Li–O pairs reveals that this interaction is again electrostatic in nature. According to the computed NBA charges for **INT<sub>d</sub>** at the HF/6-31+G\* level, the two water molecules have a bulk charge of +0.036. Coordination of the two water molecules results in a lowering of the charge at lithium, and a concomitant increase in that at the carbon atom of the nitronate, which enhances its nucleophilicity. The charge on this carbon atom is –0.221, a value between the corresponding values in **1a** and **1c**. We also located another solvated intermediate, labeled **INT'<sub>d</sub>** in Figure 7. This intermediate also exhibits a distorted tetrahedral environment for the lithium atom, but incorporates only one water molecule. Given the higher basicity of sp<sup>3</sup>-hybridized with respect to the more electronegative sp<sup>2</sup>-hybridized

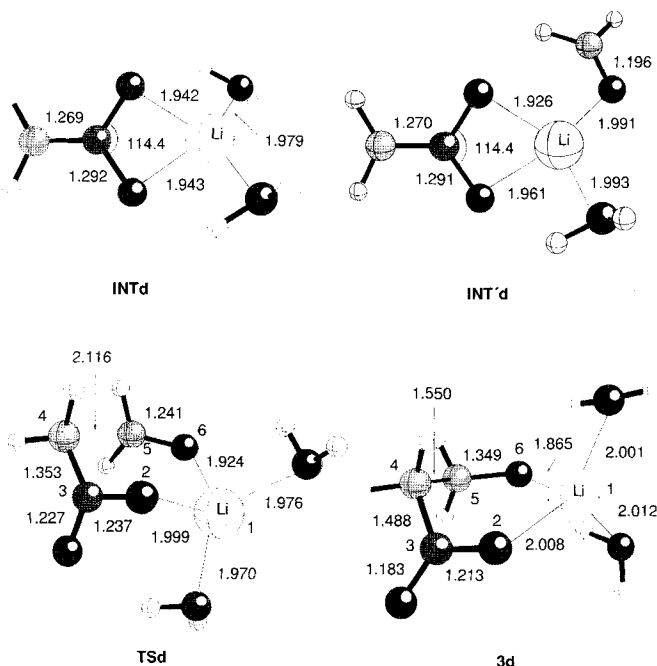


Figure 7. Fully HF/6-31+G\* optimized geometries of stationary points corresponding to reaction 4 (see Scheme 2). Bond distances and angles are given in Å and deg., respectively.

dized oxygen atoms, it was expected that the  $\text{INT}'\text{d} + \text{H}_2\text{O}$  ensemble would be less stable than  $\text{INTd} + 2\text{a}$ . This was indeed found to be the case, and our complexation energies are lower for the former intermediate than those found for the latter (Table 5). For example,  $\text{INT}'\text{d} + \text{H}_2\text{O}$  is predicted to be 1.19 kcal mol<sup>-1</sup> higher in energy than  $\text{INTd} + 2\text{a}$  at the MP4SDQ/6-31+G\*//HF/6-31+G\*+ $\Delta\text{ZPVE}$  level. Interestingly, our calculated value for  $\Delta E_c$  is  $-33.75$  kcal mol<sup>-1</sup> (MP4SDQ/6-31+G\*//HF/6-31+G\*+ $\Delta\text{ZPVE}$  results, Table 5), a value similar to the enthalpy of solvation associated with related ion–molecule clusters.<sup>[4,5]</sup>

Table 5. Differences in energy [a,b] (kcal mol<sup>-1</sup>) corresponding to reaction 4.

	HF/6-31+G*	MP2/6-31+G*// HF/6-31+G*	MP3/6-31+G*// HF/6-31+G*	MP4SDQ/6-31+G*// HF/6-31+G*
$\Delta E_c$	-28.80 [c]	-34.51 [c]	-34.02 [c]	-33.75 [c]
$\Delta E'_c$	-28.26 [d]	-33.14 [d]	-32.87 [d]	-32.56 [d]
$\Delta E_a$	+11.14	-6.02	+1.62	+1.45
$\Delta E_{\text{rxn}}$	-34.39	-51.87	-46.58	-46.66

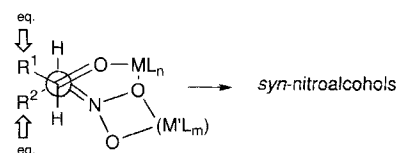
[a] See Figure 1 for the definition of energy differences. [b] Zero-point vibrational energies, scaled by 0.89 and computed at the HF/6-31+G\* level, are included. [c] Complexation energy computed as  $\Delta E_c = E(\text{INTd}) - [E(1\text{c}) + 2E(\text{H}_2\text{O})]$ . [d] Complexation energy computed as  $\Delta E'_c = E(\text{INT}'\text{d}) - [E(1\text{c}) + E(2\text{a}) + E(\text{H}_2\text{O})]$ .

The transition structure **TSd** associated with this reaction is predicted to have a chair conformation even at the HF/6-31+G\* level, with the lithium atom coordinated to two water molecules, to the oxygen atom of **2a**, and to one oxygen atom of the nitronate moiety. The C4–C5 bond order at the HF/6-31+G\* level is calculated to be of 0.374. Given the electrostatic tetracoordination of lithium and the higher nucleophilicity of **INTd**, the activation barrier is lower than that found for the

preceding reaction. The calculated value of  $\Delta E_a$  is of only +1.45 kcal mol<sup>-1</sup> at our highest level of theory (Table 5).

The O-lithiated product of this reaction is **3d** (Figure 7) in which the lithium atom has the same coordination pattern previously found for **TSd**. Again, the conformation of this reaction product is calculated to be sofa-like. The reaction energy of **3d** with respect to the nonsolvated nitronate **1c** and **2a** is  $-46.66$  kcal mol<sup>-1</sup> at our highest level of theory. However, if we consider the solvated nitronate **INTd** and **2a**, this value is only  $-12.91$  kcal mol<sup>-1</sup> and is thus comparable to that obtained in aldol reactions with presumably tetracoordinated lithium enolates.<sup>[4,41]</sup>

In summary, we can conclude that the Henry reaction between monometalated nitronates and carbonyl compounds takes place via chairlike transition states, in which the lithium atom is in a tetrahedral environment. If solvation is considered, the activation barriers are expected to be lower than those obtained for the Henry reaction involving the free nitronates. Under these conditions, stereocontrol does not appear to be very high, since important factors present in the aldol reaction (namely, bulky substituents in esters and ketones, (*E*)/(*Z*) isomerism in enolates) cannot operate here. In any case, it is expected that inclusion of bulky ligands in the coordination sphere of a metal might result in higher stereocontrol in favor of *syn*-nitroalcohols, in agreement with the results reported by Shibasaki et al.<sup>[9]</sup> The reaction would then proceed via a saddle point in which the substituents of the reactants occupy equatorial positions (*vide supra*). The general model is represented in Scheme 4.



Scheme 4. Increase in *syn* selectivity by means of metals coordinated to bulky ligands L.

**Nitromethane Lithium Lithionitronate plus Formaldehyde (Reaction 5):** This reaction was selected to model the well-known Seebach methodology involving the reaction between doubly deprotonated nitroalkanes and carbonyl compounds. The stationary points located at the HF/6-31+G\* level are depicted in Figure 8, and the corresponding relative energies are reported in Table 6.

Table 6. Differences in energy [a,b] (kcal mol<sup>-1</sup>) corresponding to reaction 5 (nitromethane lithium lithionitronate plus formaldehyde).

	HF/6-31+G*	MP2/6-31+G*// HF/6-31+G*	MP3/6-31+G*// HF/6-31+G*	MP4SDQ/6-31+G*// HF/6-31+G*
$\Delta E_c$	-16.42	-17.75	-18.07	-17.80
$\Delta E'_c$	-15.02	-15.76 [c]	-16.18 [c]	-15.95 [c]
$\Delta E_a$	+5.59 [d]	+2.18 [d]	+3.60 [d]	+3.46 [d]
$\Delta E_{\text{rxn}}$	-40.23	-44.80	-45.36	-43.35
$\Delta\Delta E_{\text{rxn}}$	+22.62 [e]	+19.64 [e]	+21.51 [e]	+20.95 [e]

[a] See Figure 1 for the definition of energy differences. [b] Zero-point vibrational energies, scaled by 0.89 and computed at the HF/6-31+G\* level, are included. [c] Complexation energy computed from **INT'e** (see Figure 8). [d] Computed as  $\Delta E_a = E(\text{TSe}) - E(\text{INT'e})$  (see text). [e] Computed as  $\Delta\Delta E_{\text{rxn}} = E(3\text{e}) - E(3\text{e})$  (see Figure 8).

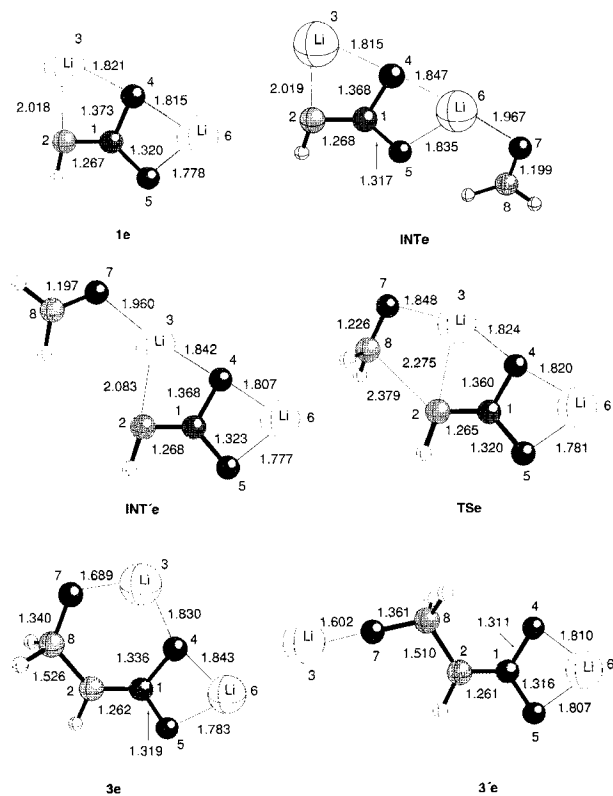


Figure 8. Fully HF/6-31+G\* optimized geometries of stationary points corresponding to reaction 5 (see Scheme 2). Bond distances are given in Å.

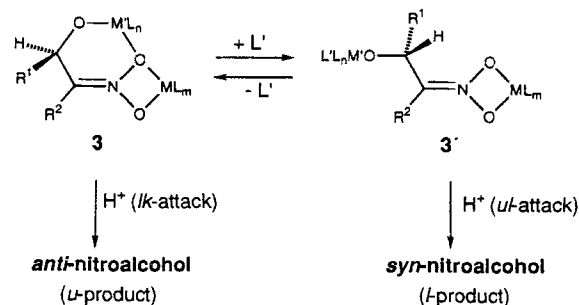
Nitromethane lithium lithionitronate (**1e**) is predicted to have a planar  $C_s$ -symmetric structure at the HF/6-31+G\* level (cf. Figure 8). The Li 3 atom is bound to both the C 2 and O 4 atoms. The analysis of the gradient of the electron density in the resulting cyclic structure reveals that there is a (3, +1) ring point corresponding to the N 1–C 2–Li 3–O 4 system. Similarly, there is another (3, +1) ring point between the O 5, N 1, O 4, and Li 6 atoms. The NBA analysis also reveals that the C 2–Li 3 bond is less electrostatic than the Li–O bonds, since for the former  $H(r_e) = +0.006$  au. The NBA charges for the Li 3 and Li 6 atoms are +0.911 and +0.946, respectively. In addition, the charge on the C 2 atom is  $-0.448$ , a value much higher than that found for nitromethane lithium nitronate (**1c**). This results in a highly nucleophilic nitronate species.

There is a local minimum in the HF/6-31+G\* energy hypersurface of this reaction, labeled **INTe** in Figure 8, in which the formaldehyde molecule is bound to the Li 6 atom. The geometrical features of this complex are similar to those found for **INTc**, with an almost linear arrangement between the two lithium–oxygen pairs. We also found another intermediate, denoted as **INT'e** in Figure 8. In this complex, the formaldehyde molecule interacts with the Li 3 atom. This intermediate is calculated to be less stable than **INTe** at all levels of theory. For example, at our highest level, **INT'e** lies  $1.85 \text{ kcal mol}^{-1}$  above **INTe** (Table 6). This result can be explained by taking into account the slightly lower charge on Li 3 than on Li 6 (vide supra); consequently, the Coulombic interaction between **1e** and **2a** is not so well stabilized in **INT'e**.

The transition structure **TSe**, leading to formation of the C 8–C 2 bond, is also depicted in Figure 8. The shape of this TS,

which has  $C_s$  symmetry, is closely related to that of **INT'e**. In addition, the IRC analysis for **TSe** connects this saddle point with **INT'e** and not with **INTe**.<sup>[27]</sup> The bond index between the C 2 and C 8 atoms is 0.282 at the HF/6-31+G\* level. In this TS, the Li 3 atom is still bound to C 2, at a distance of  $2.275 \text{ Å}$ . The angle of attack at the aldehyde, that is, the C 2–C 8–O 7 bond angle, is  $109.4^\circ$ , a normal value for addition reactions at carbonyl compounds. **TSe** is only  $3.46 \text{ kcal mol}^{-1}$  above **INT'e** at our highest level of theory. This is a much smaller value than that obtained for the reaction between **2a** and the unsolvated nitromethane lithium nitronate (**1c**) (cf. reaction 3), and can be explained in terms of the higher nucleophilicity of **1e**. This result is in agreement with the reported experimental evidence, since it has been found that doubly deprotonated nitronates are able to react with carbonyl compounds of relatively low electrophilicity such as ketones.<sup>[5]</sup>

We located two reaction products from the interaction between **1e** and **2a**. The first one is labeled **3e** in Figure 8 and has two dicoordinated lithium atoms. In particular, the Li 3 atom is bound to O 7 and O 4, thus forming a six-membered ring. The other complexed product, **3'e**, also has a plane of symmetry, but its geometry involves an antiparallel arrangement between the alkoxide and nitronate dipoles. In this latter complex, the Li 3 atom is bound only to O 7. As a consequence, its energy is significantly higher at all the levels of theory included in our study (see the  $\Delta\Delta E_{\text{rxn}}$  values in Table 6). The IRC analysis reveals that the reaction product corresponding to **TSe** is **3e**. No TS connecting **INT'e** or **INTe** with **3'e** could be located.<sup>[27]</sup> Therefore, if substituted species of type **3**, such as those represented in Scheme 5, are protonated by *lk* attack, stereoselective



Scheme 5. Possible alternative protonation pathways for alkoxide nitronates **3** and **3'** to yield *anti* and *syn*-nitroalcohols, respectively.

formation of the corresponding *anti*-nitroalcohol would be expected. This is the case when mixed silyl–lithium derivatives are used ( $M = \text{Li}$ ,  $M' = \text{Si}$ ; Scheme 5). However, in the case of dilithiated complexes ( $M = M' = \text{Li}$ ), Seebach et al. observed stereoselective formation of the corresponding *syn*-nitroalcohols.<sup>[46]</sup> These authors also noted that appropriate cosolvents such as hexamethylphosphoramide (HMPA) are required to obtain good stereocontrol. This highly coordinating additive could shift the equilibrium from **3** to **3'** ( $L' = \text{HMPA}$ , Scheme 5) thus favoring the formation of the *syn*-nitroalcohol through *ul* protonation of **3'**. Another possibility is that these complexes are preferentially protonated at oxygen ( $M = \text{H}$ , Scheme 5). In this case, the *syn*-nitroalcohol should be favored owing to intramolecular hydrogen bonding (cf. Figure 3). For silicon derivatives ( $M' = \text{Si}$ ) the *anti*-nitroalcohol would be the more stable stereoisomer.



## Conclusions

From the ab initio calculations reported in this paper, the following conclusions can be drawn:

- 1) The Henry reaction between anionic nitronates and aldehydes takes place via antiperiplanar transition states, in which the carbonyl and nitro dipoles are antiparallel to one another. This leads to the preferential formation of *anti* nitroalcohols. Substitution at both the nitronate and the carbonyl compound increases the activation barrier and the reversibility of the reaction.
- 2) The reaction between monometalated nitronates and carbonyl compounds takes place via cyclic transition structures having chairlike conformation. The favored product in this case is the *syn*-diastereomer, although effective stereocontrol is difficult. Solvation of the metal is important in order to increase the nucleophilicity of the nitronate.
- 3) The reaction with dimetalated nitronates has much lower activation barriers, and Henry reactions with less electrophilic carbonyl compounds, such as ketones, are thus possible. The *anti* or *syn* nitroalcohols should be formed preferentially depending on whether the cyclic or open metalated adducts are protonated.

**Acknowledgements.** The present work was supported by the Universidad del País Vasco/Euskal Herriko Unibertsitatea (Project UPV 170.215-EA156/94) and by the Gobierno Vasco/Eusko Jaurlaritza (Project GV 170.215-0119/94). We thank Professor J. M. Ugalde for helpful discussions and suggestions during the preparation of this work.

Received: June 17, 1996 [F 393]

- [1] L. Henry, C. R. Hebd. Scances, *Acad. Sci.* **1895**, 120, 1265.
- [2] See for example: a) S. Hanessian, J. Kloss, *Tetrahedron Lett.* **1985**, 26, 1261; b) A. G. M. Barrett, C. Robyr, C. D. Spilling, *J. Org. Chem.* **1989**, 54, 1233; c) S. Brandänge, B. Lindqvist, *Acta Chem. Scandinavica B* **1985**, 39, 589; d) H. Sasai, W.-S. Kim, T. Suzuki, M. Shibusaki, *Tetrahedron Lett.* **1994**, 35, 6123; e) V. Wöhner, V. Jäger, *Angew. Chem. Int. Ed. Engl.* **1990**, 29, 1169; f) M. Adamczyk, R. E. Reddy, *Tetrahedron Lett.* **1995**, 36, 9121; g) R. Ballini, G. Bosica, *J. Org. Chem.* **1994**, 59, 5466, and references therein; h) P. Magnus, P. Pye, *J. Chem. Soc. Chem. Commun.* **1995**, 1933; i) R. Ballini, G. Bosica, G. Ruffiani, *Helv. Chim. Acta* **1995**, 78, 879; j) R. Ballini, E. Marcantoni, M. Petrini, *Liebigs Ann.* **1995**, 1381; k) W.-C. Chou, C. Fotsch, C.-H. Wong, *J. Org. Chem.* **1995**, 60, 2916; l) Z. J. Witzczak, Y. Li, *Tetrahedron Lett.* **1995**, 36, 2595; m) R. Ballini, G. Bosica, *Synthesis* **1994**, 723; n) T. Kolter, G. van Echten-Deckert, K. Sandhoff, *Tetrahedron* **1994**, 50, 13425; o) R. Chinchilla, C. Nájera, P. Sánchez-Agulló, *Tetrahedron: Asymmetry* **1994**, 5, 1393; p) H. Sasai, T. Suzuki, N. Itoh, M. Shibusaki, *Appl. Organometallic Chem.* **1995**, 9, 421.
- [3] a) D. Seebach, E. W. Colvin, F. Lehr, T. Weller, *Chimia* **1979**, 33, 1; b) G. Rosini, R. Ballini, *Synthesis* **1988**, 833; c) R. Tamura, A. Kamimura, N. Ono, *Synthesis* **1991**, 423; d) *Nitro Compounds, Recent Advances in Synthesis and Chemistry* (Eds.: H. Fever, A. T. Nielsen), VCH, Weinheim, **1990**.
- [4] G. Rosini in *Comprehensive Organic Synthesis*, Vol. 2 (Ed. B. M. Trost), Pergamon, New York, **1991**, pp. 321–340, and refs [5–19] included therein.
- [5] a) D. Seebach, F. Lehr, *Angew. Chem. Int. Ed. Engl.* **1976**, 15, 505; b) E. W. Colvin, D. Seebach, *J. Chem. Soc. Chem. Commun.* **1978**, 689; c) D. Seebach, A. K. Beck, F. Lehr, T. Weller, E. Colvin, *Angew. Chem. Int. Ed. Engl.* **1981**, 20, 397.
- [6] R. E. Marti, J. Heinzer, D. Seebach, *Liebigs Ann.* **1995**, 1193.
- [7] G. Rosini, R. Ballini, P. Sorrenti, *Synthesis* **1983**, 1014.
- [8] a) R. Fernández, C. Gasch, A. Gómez-Sánchez, J. E. Vilchez, A. L. Castro, M. J. Diáñez, M. D. Estrada, S. Pérez-Garrido, *Carbohydr. Res.* **1993**, 247, 239; b) S. Hanessian, P. V. Devasthale, *Tetrahedron Lett.* **1996**, 37, 987.
- [9] H. Sasai, T. Tokunaga, S. Watanabe, T. Suzuki, N. Itoh, M. Shibusaki, *J. Org. Chem.* **1995**, 60, 7388. For a previous paper on lanthanum-catalyzed asymmetric Henry reaction, see ref. [2] therein.
- [10] Gaussian 92, Revision C, M. J. Frisch, G. W. Trucks, M. Head-Gordon, P. M. W. Gill, M. W. Wong, J. B. Foresman, B. G. Johnson, H. B. Schlegel, M. A. Robb, E. S. Replogle, R. Gomperts, J. L. Andres, K. Raghavachari, J. S. Binkley, C. Gonzalez, R. L. Martin, D. J. Fox, D. J. Defrees, J. Baker, J. J. P. Stewart, J. A. Pople, Gaussian, Inc., Pittsburgh PA, 1992.
- [11] Gaussian 94, Revision B.2, M. J. Frisch, G. W. Trucks, H. B. Schlegel, P. M. W. Gill, B. G. Johnson, M. A. Robb, J. R. Cheeseman, T. Keith, G. A. Petersson, J. A. Montgomery, K. Raghavachari, M. A. Al-Laham, V. G. Zakrzewski, J. V. Ortiz, J. B. Foresman, C. Y. Peng, P. Y. Ayala, W. Chen, M. W. Wong, J. L. Andres, E. S. Replogle, R. Gomperts, R. L. Martin, D. J. Fox, J. S. Binkley, D. J. Defrees, J. Baker, J. P. Stewart, M. Head-Gordon, C. Gonzalez, and J. A. Pople, Gaussian, Inc., Pittsburgh PA, 1995.
- [12] W. J. Hehre, L. Radom, P. v. R. Schleyer, J. A. Pople, *Ab Initio Molecular Orbital Theory*, Wiley, New York, **1986**, pp. 86–87, and references therein.
- [13] a) J. S. Binkley, J. A. Pople, *Int. J. Quantum Chem.* **1975**, 9, 229; b) J. A. Pople, J. S. Binkley, R. Seeger, *Int. J. Quantum Chem. Symp.* **1976**, 10, 1.
- [14] H. Hofmann, E. Hänsele, T. Clark, *J. Comput. Chem.* **1990**, 11, 1147.
- [15] a) R. G. Parr, W. Yang, *Density-Functional Theory of Atoms and Molecules*, Oxford, New York, **1989**; b) L. J. Bartolotti, K. Flurichick in *Reviews in Computational Chemistry*, Vol. 7 (Eds.: K. B. Lipkowitz, D. B. Boyd), VCH, New York, **1996**, pp. 187–216.
- [16] A. D. Becke, *J. Chem. Phys.* **1993**, 98, 5648.
- [17] a) A. D. Becke, *Phys. Rev. A* **1988**, 38, 3098; b) C. Lee, W. Yang, R. G. Parr, *Phys. Rev. B* **1980**, 37, 785; c) S. H. Vosko, L. Wilk, M. Nusair, *Can. J. Phys.* **1980**, 58, 1200.
- [18] J. A. Pople, B. Schlegel, R. Krishnan, D. J. De Fries, J. S. Binkley, H. Frisch, R. Whiteside, R. F. Hout, Jr., W. J. Hehre, *Int. J. Quantum Chem. Symp.* **1981**, 15, 269.
- [19] J. W. McIver, A. K. Komornicki, *J. Am. Chem. Soc.* **1972**, 94, 2625.
- [20] a) K. Fukui, *Acc. Chem. Res.* **1981**, 14, 363; b) C. Gonzalez, H. B. Schlegel, *J. Chem. Phys.* **1989**, 90, 2154; c) C. Gonzalez, H. B. Schlegel, *J. Phys. Chem.* **1990**, 94, 5523.
- [21] K. B. Wiberg, P. R. Rabien, *J. Comput. Chem.* **1993**, 14, 1504.
- [22] K. B. Wiberg, *Tetrahedron* **1968**, 24, 1083.
- [23] a) A. E. Reed, R. B. Weinstock, F. Weinhold, *J. Chem. Phys.* **1985**, 83, 735; b) A. E. Reed, L. A. Curtiss, F. Weinhold, *Chem. Rev.* **1988**, 88, 899; c) A. E. Reed, P. von R. Schleyer, *J. Am. Chem. Soc.* **1990**, 112, 1434.
- [24] R. F. W. Bader, *Atoms in Molecules—A Quantum Theory*, Clarendon Press, Oxford, **1990**.
- [25] F. W. Biegler-König, R. F. W. Bader, T. Tang, *J. Comput. Chem.* **1982**, 3, 317.
- [26] K. B. Wiberg, H. Castejon, *J. Org. Chem.* **1995**, 60, 6327.
- [27] We are grateful to one of the referees for suggesting this computation.
- [28] Y. Li, M. N. Paddon-Row, K. N. Houk, *J. Org. Chem.* **1990**, 55, 481.
- [29] K. N. Houk, Y. Li, J. D. Evanseck, *Angew. Chem. Int. Ed. Engl.* **1992**, 31, 682.
- [30] a) H. B. Bürgi, J.-M. Lehn, G. Wipff, *J. Am. Chem. Soc.* **1974**, 96, 1956; b) H. B. Bürgi, J. D. Dunitz, J.-M. Lehn, *Tetrahedron* **1974**, 30, 1563.
- [31] In contrast, **TSb(anti)** is predicted to be 1.36 kcal mol<sup>-1</sup> more stable than **TSb(syn)** at the HF/3-21G(\*) level.
- [32] M. E. Flanagan, J. R. Jacobsen, E. Sweet, P. G. Schultz, *J. Am. Chem. Soc.* **1996**, 118, 6078.
- [33] H. Bock, R. Dienelt, H. Schödel, Z. Havias, *Tetrahedron Lett.* **1995**, 36, 7855.
- [34] G. Klebe, K. H. Böhn, M. Marsch, G. Boche, *Angew. Chem., Int. Ed. Engl.* **1987**, 26, 78.
- [35] a) F. Bernardi, A. Bongini, G. Cainelli, M. A. Robb, G. S. Valli, *J. Org. Chem.* **1993**, 58, 750; b) M. J. S. Dewar, K. Merz, *J. Am. Chem. Soc.* **1987**, 109, 6553.
- [36] D. Cremer, E. Craka, *Croat. Chim. Acta* **1984**, 57, 1259.
- [37] For a recent example on the application of the  $H(r_c)$  criterion in ion–molecule clusters see X. Lopez, J. M. Ugalde, F. P. Cossio, *J. Am. Chem. Soc.* **1996**, 118, 2718.
- [38] For an excellent review in the gegenion effects on alkali organometallic compounds, see C. Lambert, P. von R. Schleyer, *Angew. Chem. Int. Ed. Engl.* **1994**, 33, 1129.
- [39] C. Lambert, Y.-D. Wu, P. von R. Schleyer, *J. Chem. Soc. Chem. Commun.* **1993**, 255.
- [40] R. Leung-Toung, T. T. Tidwell, *J. Am. Chem. Soc.* **1990**, 112, 1042.
- [41] P. G. Williard, G. B. Carpenter, *J. Am. Chem. Soc.* **1986**, 108, 462.
- [42] a) J. E. Del Bene, M. J. Frisch, K. Raghavachari, J. A. Pople, P. von R. Schleyer, *J. Phys. Chem.* **1983**, 87, 73; b) S. Shambayati, S. L. Schreiber in *Comprehensive Organic Synthesis*, Vol. 5 (Eds.: B. M. Trost, I. Fleming), Pergamon, Oxford, 1991; pp. 283–324.
- [43] Y. Li, M. N. Paddon-Row, K. N. Houk, *J. Am. Chem. Soc.* **1988**, 110, 3684.
- [44] For example, Arnett et al. reported the calorimetric determination of the reaction enthalphy associated with the aldol reaction between the lithium enolate of pinacolone and pinaldehyde. Their value for  $\Delta H_{rxn}$  is  $-30.2$  kcal mol<sup>-1</sup> in hexane and  $-19.0$  kcal mol<sup>-1</sup> in DME (two oxygen atoms available for coordination). See: D. Seebach, *Angew. Chem. Int. Ed. Engl.* **1988**, 27, 1624, and ref. [164] therein.
- [45] For example, the experimental enthalpy for the process  $\text{Li}(\text{H}_2\text{O})_2^+ + 2\text{H}_2\text{O} \rightarrow \text{Li}(\text{H}_2\text{O})_4^+$  is  $\Delta H^\circ = -37.1$  kcal mol<sup>-1</sup>. See, R. G. Keese, A. W. Castleman, Jr., *J. Phys. Chem. Ref. Data* **1986**, 15, 1011.
- [46] a) M. Eyer, D. Seebach, *J. Am. Chem. Soc.* **1985**, 107, 3601; b) D. Seebach, A. K. Beck, T. Mukhopadhyay, E. Thomas, *Helv. Chim. Acta* **1982**, 65, 1101.